

## EPIC 228782059: Asteroseismology of what could be the coolest pulsating helium-atmosphere white dwarf (DBV) known?

R.M. DUAN,<sup>1</sup> W. ZONG,<sup>1</sup> J.-N. FU,<sup>1</sup> Y.H. CHEN,<sup>2</sup> J. J. HERMES,<sup>3</sup> ZACHARY P. VANDERBOSCH,<sup>4</sup> X.Y. MA,<sup>1</sup> AND S.CHARPINET<sup>5</sup>

<sup>1</sup>*Department of Astronomy, Beijing Normal University, Beijing 100875, P. R. China*

<sup>2</sup>*Institute of Astrophysics, Chuxiong Normal University, Chuxiong 675000, P. R. China*

<sup>3</sup>*Department of Astronomy & Institute for Astrophysical Research, Boston University, 725 Commonwealth Ave., Boston, MA 02215, USA*

<sup>4</sup>*Department of Astronomy, The University of Texas at Austin, Austin, TX 78712, USA*

<sup>5</sup>*Institut de Recherche en Astrophysique et Planétologie, CNRS, Université de Toulouse, CNES, 14 Avenue Edouard Belin, 31400 Toulouse, France*

(Received —; Revised —; Accepted —)

Submitted to ApJ

### ABSTRACT

We present analysis of a new pulsating helium-atmosphere (DB) white dwarf, EPIC 228782059, discovered from 55.1 days of *K2* photometry. The long duration, high quality light curves reveal 11 independent dipole and quadruple modes, from which we derive a rotational period of  $34.1 \pm 0.4$  hr for the star. An optimal model is obtained from a series of grids constructed using the White Dwarf Evolution Code, which returns  $M_* = 0.685 \pm 0.003 M_\odot$ ,  $T_{\text{eff}} = 21,910 \pm 23$  K and  $\log g = 8.14 \pm 0.01$  dex. These values are comparable to those derived from spectroscopy by Koester & Kepler ( $20,860 \pm 160$  K and  $7.94 \pm 0.03$  dex). If these values are confirmed or better constrained by other independent works, it would make EPIC 228782059 one of the coolest pulsating DB white dwarf star known, and would be helpful to test different physical treatments of convection, and to further investigate the theoretical instability strip of DB white dwarf stars.

*Keywords:* asteroseismology-star: individual: EPIC228782059, DB type, white dwarf

### 1. INTRODUCTION

White dwarfs mark the graveyard and evolutionary destiny for all low-mass stars when nuclear burning ceases fire in their cores. About 98% of stars in our Galaxy will evolve into white dwarfs (Winget & Kepler 2008), including our Sun. These faint blue stars offer extreme conditions to test fundamental physics that is far from reach by the current terrestrial laboratory (see, e.g., Kritcher et al. 2020; Niu et al. 2018). They can also be the tracer to ages for cosmology and Galactic archaeology (Fontaine et al. 2001).

When white dwarfs evolve along cooling tracks, they go through several different regions where they pulsate, mainly the DOV, DBV and DAV instability strips. As they cool, their brightness can be modulated as the result of convection-driven pulsations (see, e.g., Winget & Kepler 2008; Fontaine & Brassard 2008; Althaus et al. 2010, and reference therein).

Among all types of pulsating white dwarfs, the DBV (or V777 Her) class refers to those with helium-dominated at-

mospheres, ranging from roughly  $22,000 < T_{\text{eff}} < 32,000$  K and  $7.5 < \log g < 8.3$  dex (Córscico et al. 2019). The first DBV was discovered immediately following the theoretical prediction of its existence by Winget et al. (1982). We now know of roughly 40 DBV stars, which is about 11% of all pulsating white dwarfs known (Córscico et al. 2019; Vanderbosh et al. 2018).

The richness of pulsations in non-radial  $g$ -modes offers a new window to probe the interior structure and chemical profiles of a DBV star (see, e.g., Robinson et al. 1982). In order to produce better frequency resolution in pulsation spectra for DBV observations, a global network called the Whole Earth Telescope (see, e.g., Nather et al. 1990) was organized in order to collect photometric data for several particular interesting DBVs, such as GD 358 (see, e.g., Kepler et al. 2003). With its numerous pulsations observed, GD 358 has been explored for various physical tests of convection, magnetism, and rotation (Provencal et al. 2009; Montgomery et al. 2010). The long-term observations of DBV stars may also provide constraints of the cooling rate of hot white dwarfs, where neutrinos contribute meaningfully to the luminosity (Winget et al. 2004).

The *Kepler* mission delivered unprecedented, high-quality photometric data, leading to various breakthroughs in stellar physics, in particular, probing the internal physical processes of pulsating stars via the technique of asteroseismology (see, e.g., [Giammichele et al. 2018](#); [Córscico 2020](#)). There was only one DBV star, KIC 08626021, discovered with multiple pulsations in the original *Kepler* field ([Østensen et al. 2011](#)). Due to its precise frequency resolution, it has been the subject of intensive studies to improve theoretical models, such as those of the parametric evolutionary models of the White Dwarf Evolution Code (WDEC; [Bischoff-Kim & Montgomery 2018](#)) and the fully evolutionary models of the La Plata code (LPCODE; [Córscico et al. 2013](#)), where the latter harbors chemical structures resulting from the complete evolutionary history of the progenitor stars.

With further observations by *Kepler*, [Bischoff-Kim et al. \(2014\)](#) identified seven independent modes to re-construct the WDEC model for KIC 08626021, revealing a very thin helium layer and hot temperature. Additionally, [Zong et al. \(2016\)](#) discovered clear amplitude and frequency modulations occurring in several multiplets in that star using the same data. They attribute those modulations to nonlinear mode interactions, which lead to identification of one additional independent mode. With eight modes, [Giammichele et al. \(2018\)](#) performed a static forward model to KIC 08626021 and obtained an unprecedentedly precise solution, measuring a large core with a higher oxygen-to-carbon ratio than previous solutions. The results were challenged by [Timmes et al. \(2018\)](#), who suggested that neutrino cooling would also impact the seismic solution to KIC 08626021 at such a high effective temperature. A quick response by [Charpinet et al. \(2019a\)](#) suggested that the neutrino emission, indeed, should be incorporated in the static models, but does not have a significant effects on the seismic properties derived for KIC 08626021. Nevertheless, [De Gerónimo et al. \(2019\)](#) conclude that the current white dwarf formation and evolution can hardly reproduce the internal chemical results of KIC 08626021 derived by [Giammichele et al. \(2018\)](#).

After a failure of the second reaction wheel controlling pointing of the spacecraft, *Kepler* began observations of new campaigns along the ecliptic plane ([Howell et al. 2014](#)). This strategy, also called the *K2* mission, produced more white dwarfs to be monitored, enabling observations of many more pulsating white dwarfs ([Hermes et al. 2017b](#)). To date, only one DBV observed by *K2* has been published. That DBV, PG 0112+104, has stable pulsation frequencies and a rotation period of 10.2 hr ([Hermes et al. 2017a](#)).

Here we report the discovery of a new DBV star, EPIC 228782059, located near the cool edge of the DBV instability strip. The paper is organised as follows: In Section 2 we describe *K2* photometry and frequency content for

EPIC 228782059. We present the seismic results from the WDEC code and discuss its location in the DBV instability strip in Section 3. The conclusion is given in the final section.

## 2. FREQUENCY CONTENT

### 2.1. Photometry

EPIC 228782059 (SDSS J124538.21-073138.3,  $K_p = 18.4$  mag, Figure 1a) was identified as a DB-type white dwarf from the Sloan Digital Sky Survey (SDSS) by [Kleinman et al. \(2013\)](#). An analysis of atmospheric parameters of DBs from the SDSS found for this star  $T_{\text{eff}} = 20,868 \pm 160$  K and  $\log g = 7.914 \pm 0.027$  dex ([Koester & Kepler 2015](#)). EPIC 228782059 was proposed to be observed by *K2* in Campaign 10. The target pixel files (TPFs) in short-cadence (58.85 s) were downloaded from the Mikulski Archive for Space Telescopes, and we use the *Lightkurve* ([Lightkurve Collaboration et al. 2018](#)) package to extract photometry from the TPFs. As *K2* suffers a  $\sim 6.5$  hr thruster firing to compensate for the solar pressure variation for fine pointing, we subsequently used the KEPSFF routine ([Vanderburg & Johnson 2014](#)) to correct the systematic photometric variation that is induced by the low-frequency motion of the target on the CCD module. A series of apertures of different pixel sizes were tested on the TPF to optimise the photometry. We finally chose a fixed six-pixel aperture to extract our light curve, as shown in Figure 1(b).

After extracting the photometry we fit out a third-order polynomial and sigma clipped the light curve to  $4.5\sigma$  in order to detrend the light curve and to clip the outliers, leaving 79,378 data points. Figure 1(c) shows the final light curve of EPIC 228782059 during C10 with a duration of 55.1 days. We note that there is a large gap about a week into the light curve due to the failure of CCD Module 4 during *K2* Campaign 10.

### 2.2. Frequency analysis

The flexible software package FELIX<sup>1</sup> was used for Fourier decomposition of the light curve, which incorporates the standard prewhitening and nonlinear least-square fitting techniques for Fourier transformation ([Deeming 1975](#); [Scargle 1982](#)). The threshold of acceptance for a significant frequency is set to be  $4.8\sigma$  of the local noise level, tuned from previous work with *Kepler* and *TESS* ([Zong et al. 2016](#); [Charpinet et al. 2019b](#)). Table 1 lists the frequencies with their attributes extracted with *Felix*: the ID ordered by their frequency (Column 1), frequency (Column 2), amplitude (Column 7) and their uncertainties (Column 3 and 8),

<sup>1</sup> Frequency Extraction for Lightcurve exploitation, which was developed by Stéphane Charpinet. See details of the code in [Charpinet et al. \(2010\)](#).

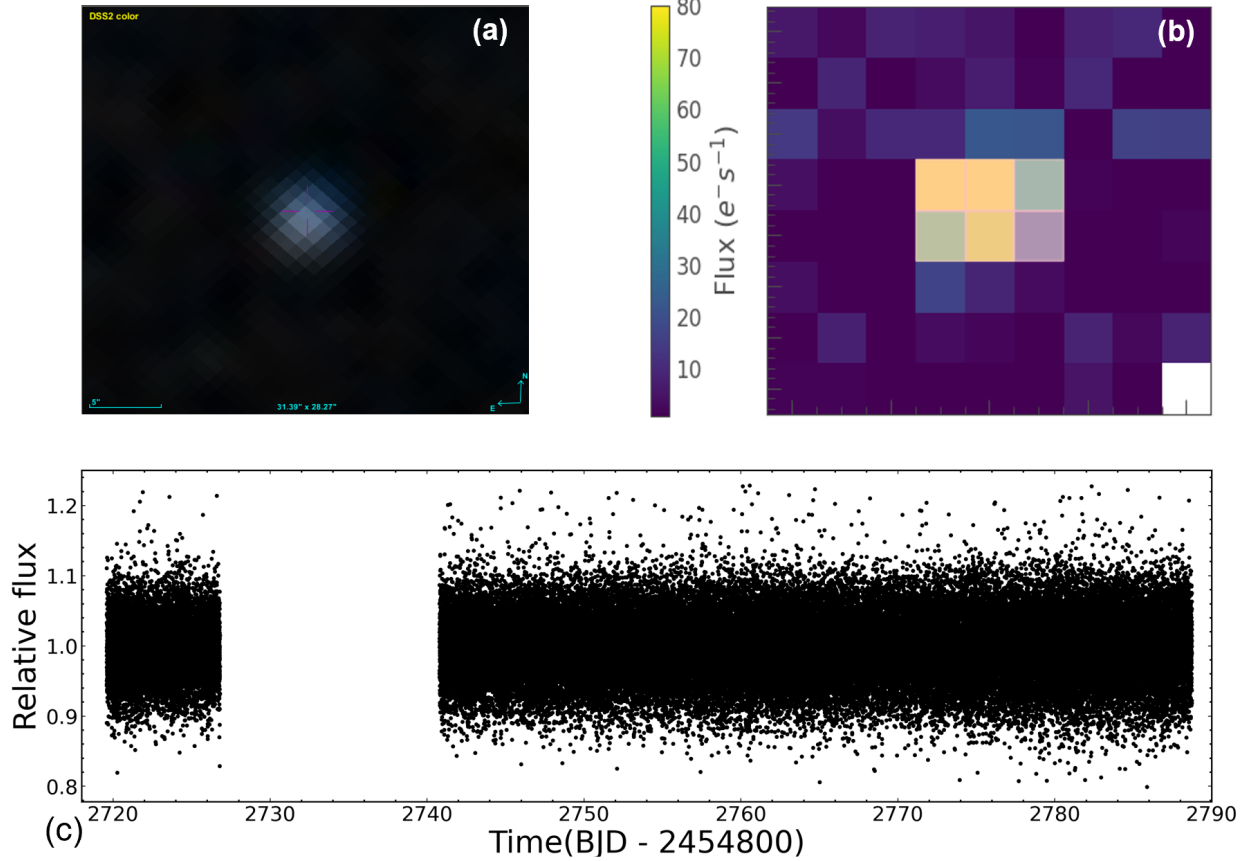


**Figure 1.** (a) The finder chart of EPIC 228782059 from Aladin and (b) the image from the *Kepler* target pixel file with the optimal aperture marked. (c) The relative flux of *K2* photometry for EPIC 228782059, with motion-correlated systematic trends removed.

the corresponding period (Column 4), the signal-to-noise ratio (SNR, Column 9), and the other quantities derived from seismic models.

Figure 2 shows the Lomb-Scargle periodogram of EPIC 228782059: significant signals are found from roughly 1500–6300  $\mu\text{Hz}$ . There are 11 frequencies detected and two additional linear combination frequencies. We note that two frequencies detected are below the significance threshold but their positions correspond well to equally spaced rotational components. The narrow profile of the rotational multiples  $f_{1,0} = 2922.5 \mu\text{Hz}$ ,  $f_{3,0} = 3432.7 \mu\text{Hz}$ ,  $f_{4,0} = 3777.9 \mu\text{Hz}$ ,  $f_{5,0} = 4358.8 \mu\text{Hz}$  are shown in the lower panels. Two values of equal frequency spacing are identified, i.e.,  $\approx 4.0 \mu\text{Hz}$  and  $\approx 6.8 \mu\text{Hz}$  for  $\ell = 1$  and  $\ell = 2$ , respectively, according to the rotational formulae that is truncated to the first order for slow rotation (see, e.g., Dziembowski & Goode 1992),

$$\omega_{nlm} = \omega_{nl} + m(1 - C_{nl})\Omega. \quad (1)$$

Here  $\omega_{nlm}$  is the rotational splitting frequency,  $\omega_{nl}$  is the non-rotational split frequency,  $\Omega$  is the rotational frequency, and

the Ledoux constant  $C_{nl} \approx 1/\ell(\ell + 1)$  for high radial-order  $g$ -modes.

### 2.3. Astroseismological analysis

Mode identification, obtained from observational constraints, is crucial to determine the seismic solutions for various theoretical models. As indicated from Equation (1), the rotational splitting frequencies provide a conventional way to identify the spherical harmonic degree  $\ell$  and the azimuthal order  $m$ . For  $g$ -mode pulsations in chemically homogeneous and radiative white dwarfs, the consecutive, higher radial orders ( $n \gg \ell$ ) follow a pattern of equal period spacing, following approximately the asymptotic regime (Tassoul et al. 1990), which depends only on the structure of a model:

$$\Delta\Pi_l \approx \frac{\Pi_0}{\sqrt{l(l+1)}} \quad (2)$$

with  $\Pi_0$  defined as,

$$\Pi_0 = 2\pi^2 \left( \int_1^R \frac{N}{r} dr \right)^{-1} \quad (3)$$

**Table 1.** The frequency content detected from K2 photometry and their mode identification in EPIC 228782059.

ID	Freq. ( $\mu\text{Hz}$ )	$\sigma$ Freq. ( $\mu\text{Hz}$ )	$P_{\text{obs}}$ (s)	$P_{\text{cal}}$ (s)	$P_{\text{obs}} - P_{\text{cal}}$ (s)	Amplitude (ppt)	$\sigma$ Amp (ppt)	SNR	$\ell$	$m$	$n$
$f_{1,0}^\dagger$	2922.545	0.002	342.167	342.388	-0.221	13.05	0.27	48.7	1	0	6
$f_{1,+1}^*$	2926.592	0.030	341.694			0.81	0.27	3.1	1	1	...
$f_{2,0}^\dagger$	2927.373	0.009	341.603	341.460	0.143	2.78	0.26	10.4	2	0	12
$f_{3,-1}$	3428.662	0.010	291.658			2.31	0.26	8.9	1	-1	...
$f_{3,0}$	3432.711	0.019	291.314	291.345	-0.031	1.26	0.26	4.9	1	0	5
$f_{3,+1}$	3436.662	0.005	290.979			4.95	0.26	19.0	1	1	...
$f_{4,-1}$	3773.867	0.016	264.980			1.52	0.26	5.8	1	-1	...
$f_{4,0}$	3777.989	0.018	264.691	264.645	0.046	1.33	0.26	5.0	1	0	4
$f_{4,+1}^*$	3782.053	0.026	264.406			0.93	0.26	3.5	1	1	...
$f_{5,-2}$	4345.170	0.009	230.140			2.66	0.26	10.1	2	-2	...
$f_{5,-1}$	4351.986	0.013	229.780			1.88	0.26	7.1	2	-1	...
$f_{5,0}$	4358.875	0.011	229.416	229.532	0.116	2.20	0.26	8.0	2	0	7
$f_{5,+2}$	4372.535	0.009	228.700			2.79	0.26	10.6	2	2	...
$\chi$					0.131						
Linear	Combinations	Frequencies									
$f_{1,0} + f_{3,+1}$	6369.216	0.017	157.252			1.43	0.27	5.4	...	...	...
$f_{5,-2} - f_{1,0}$	1422.572	0.013	702.952			1.92	0.26	7.4	...	...	...

<sup>†</sup>The  $m = 0$  identified with the minimum frequency difference between the observation and seismic models.

\*Frequencies below the  $4.8\sigma$  detection limits but consistent with the mode identification from seismic models.

where  $N$  is the Brunt-Väisälä frequency and  $r$  is the radial coordinate.

A complete triplet is found at  $3432 \mu\text{Hz}$  with three components with frequency spacing of  $\Delta f \sim 4.0 \mu\text{Hz}$ . Another triplet is resolved at  $3778 \mu\text{Hz}$  with  $\Delta f \sim 4.1 \mu\text{Hz}$ , but the prograde component ( $m = +1$ ) is below the detection threshold. A doublet is identified at  $2922.5 \mu\text{Hz}$  with a suspected prograde component whose  $m$  could be determined by a nearby peak significantly found at  $2927.3 \mu\text{Hz}$ . An incomplete quintuplet is discovered near  $4560 \mu\text{Hz}$ , with four significant components, but the  $m = +1$  one is missing, with a frequency spacing of  $\Delta f \approx 6.8 \mu\text{Hz}$ . With those identified frequency splittings, we estimate a rotation period of  $34.1 \pm 0.4$  hr for EPIC 228782059.

From the above triplets with periods at  $342.2$  s,  $291.3$  s and  $264.7$  s, we calculate a preliminary period spacing  $\Delta \Pi_1 = 25.7$  s for  $\ell = 1$  modes from the linear relationship of  $\Pi_{1,n} = 25.7 \times n + 239.4$ . The  $\ell = 2$  modes have a period spacing  $\Delta \Pi_2 = 14.8$  s, derived from  $\Delta \Pi_2 = 1/\sqrt{3}\Delta \Pi_1$ . However, this relation is only accurate for high-order modes typically with long period,  $P > 500$  s (Brassard et al. 1992). Our preliminary calculation suggests that the mode at  $2927 \mu\text{Hz}$  is very possibly identified as  $\ell = 2$ , since it is very close to the peak at  $2922 \mu\text{Hz}$ , which is the central component of an

incomplete triplet. We do not identify the two linear combination frequencies since they could be resonant modes (Zong et al. 2016) or pure non-linear effects of the flux perturbation (Brassard et al. 1995).

### 3. THEORETICAL RESULTS

#### 3.1. Asteroseismic models

With the above identifications for the observed modes of  $f_{1,0}$ ,  $f_{2,0}$ ,  $f_{3,0}$ ,  $f_{4,0}$ , and  $f_{5,0}$ , those five modes (three  $\ell = 1$  and two  $\ell = 2$ ) are used to constrain the theoretical models using the White Dwarf Evolution Code (WDEC; Lamb & van Horn 1975; Bischoff-Kim & Montgomery 2018). The latest version of WDEC incorporates the physical input parameters from the code of Modules for Experiments in Stellar Astrophysics (MESA; Paxton et al. 2011; Paxton 2019). The input parameters are crucial to the stellar structure of the build models. There are six most important parameters that can be modified in WDEC: the mass ( $M_*$ ); the effective temperature ( $T_{\text{eff}}$ ); the location of the base of the envelope ( $M_{\text{env}}$ ); the location of the helium atmosphere ( $M_{\text{He}}$ ); the helium abundance in the mixed region ( $X_{\text{He}}$ ); and the central core oxygen abundance ( $X_{\text{O}}$ ) that is determined by six parameters ( $[h_i, w_i]$  and  $i = 1, 2, 3$ ). These parameters describe the shape of the  $X_{\text{O}}$  profile, which is illustrated in Figure 3. A monotonous

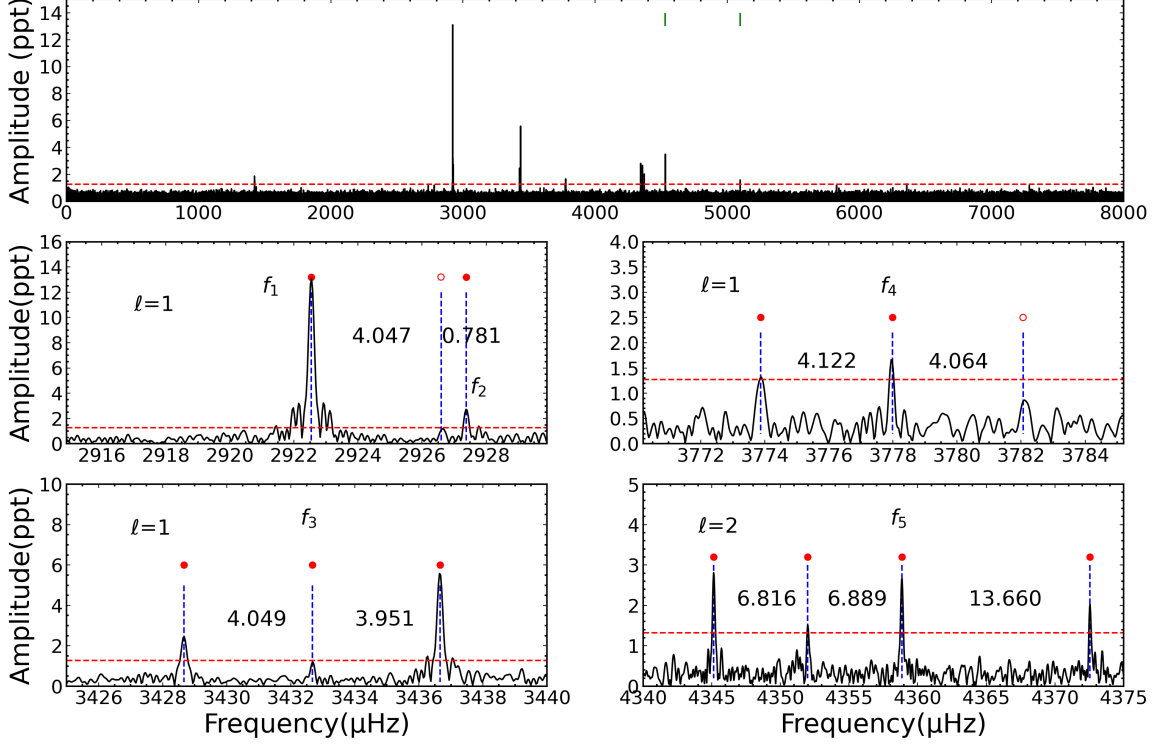


**Figure 2.** The Lomb-Scargle periodogram of EPIC 228782059. The horizontal lines (in red) denote the  $4.8\sigma$  significance threshold. Two vertical short segments indicate where the instrumental artifacts at integer harmonics of the long-cadence exposure time are identified (top panel). The solid points represent the frequencies detected above the  $4.8\sigma$  threshold, whereas the open circles are lower than  $4.8\sigma$  but probably the real ones indicated by their frequency spacing (number in lower panels). The modal degree numbers are given by their frequency spacing values.

**Table 2.** Parameter space explored by the WDEC code during optimization for EPIC 228782059.

Parameters	Range	Crude	Fine	Sophisticated	Optimal
$M_*/M_\odot$	[0.550,0. 850]	0.010	0.005	0.005	$0.685\pm 0.003$
$T_{\text{eff}}(\text{K})$	[20000, 32000]	200	50	10	$21910\pm 23$
$-\log(M_{\text{env}}/M_*)$	[2.00,5.00]	1.00	0.03	0.01	$2.11\pm 0.03$
$-\log(M_{\text{He}}/M_*)$	[3.00,6.00]	1.00	0.03	0.01	$2.91\pm 0.02$
$X_{\text{He}}$	[0.00,1.00]	0.20	0.03	0.01	$0.59\pm 0.05$
Initial $X_{\text{O}}$ (%)					
$h_1 = 62$	[50,74]	3	1	1	$52\pm 7$
* $h_2 = 68$	[59,77]	3	1	1	$61\pm 4$
* $h_3 = 83$	[77,89]	3	1	1	$78\pm 12$
$w_1 = 38$	[29,44]	3	1	1	$38\pm 1$
$w_2 = 51$	[42,57]	3	1	1	$51\pm 1$
$w_3 = 9$	[6,12]	3	1	1	$9\pm 1$

Notes.  $M_{\text{env}}$  is envelope mass ;  $M_{\text{He}}$  is helium mass ; \* The value of  $h_{j+1}$  is scaled to  $h_j$  here  $j = 1, 2$

decrease in the oxygen abundance is forced by setting the vertical height parameters to obey  $h_1 > h_2 > h_3$ . While the width parameters  $w_1, w_2, w_3$  define the mass fraction of each segment corresponding to  $h_1, h_2, h_3$ , respectively.

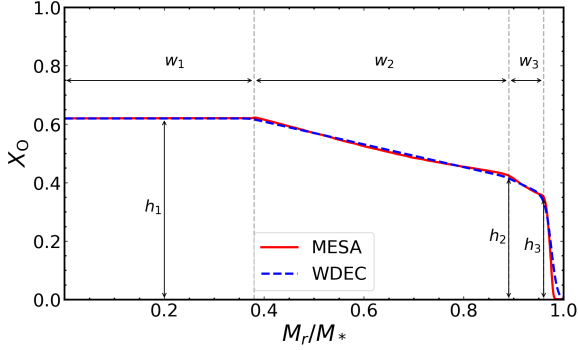


**Figure 3.** Chemical profiles of oxygen as a function of the mass coordinate.

We first evolve a main sequence star with  $3.50 M_\odot$  down to a white dwarf with  $0.65 M_\odot$  via the MESA code 8118 using default parameters. This process provides a preliminary interior  $X_O$  which was then adjusted slightly to accommodate the white dwarf models that will be calculated for eigenfrequencies by the WDEC code. Figure 3 presents the result of oxygen profile obtained by MESA and the initial parameterized  $X_O$  with  $h_1 = 0.62$ ,  $h_2 = 0.68h_1$  and  $h_3 = 0.83h_2$ . As an alternative, we change the  $X_O$  slightly to better constrain the optimal models, for instance,  $h_1 \in [0.50, 0.74]$  as listed in Table 2. As suggested by spectroscopy, the  $T_{\text{eff}}$  was set to be in the range of  $[20,000, 32,000]$  K with a rough step of 200 K, to fully cover the entire region of DBV strip. The other parameters were set in a space of a typical DB white dwarf, as listed in Table 2.

We then calculated a series of models to reproduce the observed frequencies. The quality of the fitting is evaluated quantitatively by a merit function, defined as:

$$\chi^2 = \frac{1}{N} \sum_{i=1}^N (P_{\text{cal}} - P_{\text{obs}})^2, \quad (4)$$

where  $P_{\text{cal}}$  and  $P_{\text{obs}}$  are the calculated and the observed period, respectively. Here  $N$  is the number of the independent modes with  $m = 0$ , which is five for EPIC 228782059.

We can quickly locate the good models in the parameter space using large steps, followed by finer steps in a narrower range of the better models. The optimal model was searched using more sophisticated steps. One can see the detailed values of those steps in Table 2. The seismic model revealed for EPIC 228782059 has  $T_{\text{eff}} = 21910 \pm 23$  K, roughly consistent with that derived from the SDSS spectrum (Koester & Kepler 2015). The mass is constrained from asteroseismology to be

$0.685 \pm 0.003 M_\odot$ . The period discrepancy has a value of  $\chi = 0.131$  s between the observed values and theoretical values (see individual periods in Table 1). With transformation of luminosity to magnitude, we note that the optimal seismic luminosity is  $L = 0.028 L_\odot$ , corresponding to a seismic distance of 343.56 pc, which is consistent with the result derived from the *Gaia* distance  $372.38^{+33.81}_{-29.34}$  pc (Bailer-Jones et al. 2021). Figure 4 presents the chemical composition profiles of  $X_O$ , carbon ( $X_C$ ) and helium ( $X_{\text{He}}$ ) as well as the corresponding Brunt-Väisälä frequency. We can see small bumps arising at the zones of element transition. However, our models are limited to central C/O profiles and do not incorporate other chemical elements such as  $^{22}\text{Ne}$ . Chidester et al. (2021) suggest that the presence of  $^{22}\text{Ne}$  might lead to a systematic offset of pulsation period in the fitting process of specific white dwarfs.

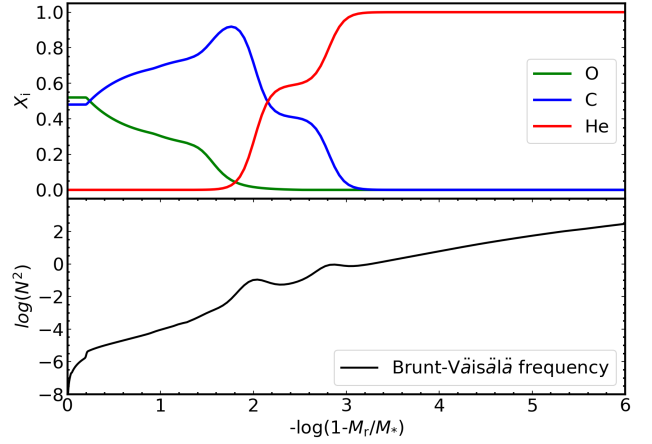


**Figure 4.** Top panel: Chemical composition profiles of oxygen, carbon and helium as a function of the outer mass fraction from our seismic model. Bottom panel: The corresponding logarithm of the squared Brunt-Väisälä frequency

### 3.2. Instability strip

Contrary to its cousin, the hydrogen-atmosphere DAV stars, there are far fewer DBV stars with detected pulsations, and DBVs account for a small fraction of all pulsating white dwarf stars known (Córscico et al. 2019). Thus the determination of the instability strip has attracted less attention for the DBVs. However, the number of DBV stars is still increasing, with many intensive observational efforts (see, e.g., Vanderbosch et al. 2018).

Given our optimal asteroseismic model, we can locate the position of EPIC 228782059 on the Kiel diagram ( $T_{\text{eff}}$  v.s.  $\log g$ ), with the determination of  $\log g$  of 8.14 dex (Figure 5). Along with the other 24 known DBV stars with derived parameters, EPIC 228782059 sits very near the red edge of the DBV instability strip, whereas the other *K2* helium-atmosphere pulsator, PG 0112+104, represents the hottest

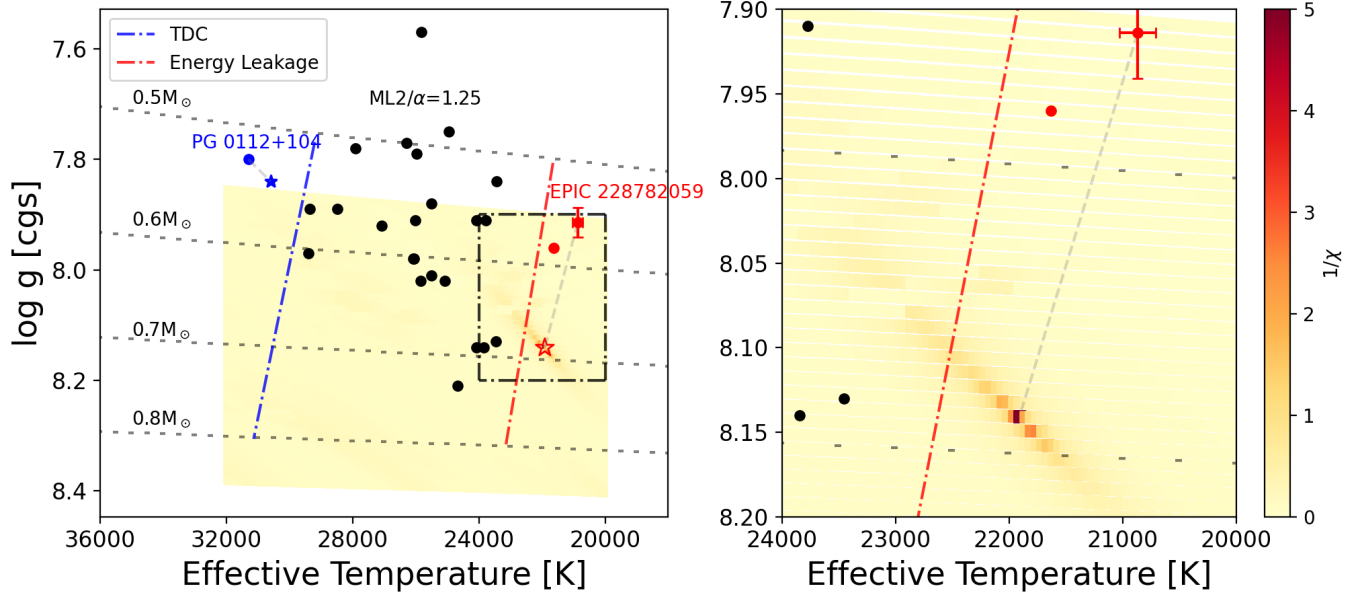


**Figure 5.** The location of EPIC 228782059, marked as a red square, in the DBV instability strip. All filled circles represent DB variables and the “star” symbol is linked to the same star but its parameters were derived from seismic model. The shadow region covers the parameter space where the WDEC code has been explored. The right panel is the expanded view of the area covered by the dashed box in the left panel. The blue and red dashed lines indicate the two edges that are calculated with different theoretical treatments (see details in text).

known DBV (Hermes et al. 2017a). As an observational constraint to the DBV instability strip, we also adopt the theoretical calculations by Van Grootel et al. (2017) with several different treatments<sup>2</sup> in four different cooling tracks of 0.5, 0.6, 0.7 and  $0.8M_{\odot}$ . We note that the evolutionary tracks in Figure 5 are slightly different to theirs since the calculations are performed by different codes with the same input parameters, i.e., the mixing length value  $ML2/\alpha = 1.25$ .

We see that most of the known DBV stars reside well within the theoretical instability strip except for PG 0112+104, the hottest one, as well as EPIC 228782059 and SDSS J102106.69+082724.8, the two coolest ones, which are important to constrain the location of the blue and red edge, respectively. PG 0112+104 stands about 1000 K hotter than the blue edge by the TDC treatment. However, Córscico et al. (2009) explored the different values of mixing length to determine the location of the blue edge and found that  $ML3/\alpha = 2$  can reproduce a blue edge to fully include PG 0112+104. Detailed calculations give a roughly 1000 K cooler red edge when energy leakage is taken into consideration (see details in Van Grootel et al. 2017). This is favored except that the two cool DBV stars were measured with a large uncertainty in  $T_{\text{eff}}$  and  $\log g$ .

Strong evidence is provided from the fact that  $T_{\text{eff}} < 22,000$  K is independently derived both from spec-

troscopy and asteroseismology using the WDEC code for EPIC 228782059. The seismic  $T_{\text{eff}}$  determination is measured based on a pure helium atmosphere (Koester & Kepler 2015). The presence of a small fraction of hydrogen may have a large effect on the determination of  $T_{\text{eff}}$ , as suggested by Bergeron et al. (2011), who claim the DBV instability strip could actually be divided into two regions, named DB and DBA instability strip, taking the hydrogen in atmosphere into account. The theoretical calculations by Van Grootel et al. (2017) do not find this distinction. The fits of Koester & Kepler (2015) put an upper limit on the detection of hydrogen in EPIC 228782059 of  $\log N(\text{H})/N(\text{He}) < -4.2$ .

However, the relative short pulsation periods disclosed here, 228.7–342.2 s, are comparable to many hot DBVs, for instance KIC 08626021 and PG 0112+104, where they typically develop shallower convection zones than cooler ones, driving shorter-period pulsations. The SDSS spectrum had also been independently analysed by Kong et al. (2018) who obtained significantly different parameters:  $T_{\text{eff}} = 29776 \pm 258$  K and  $\log g = 7.88 \pm 0.014$  dex. But this result converts into a distance of  $561.3^{+13.1}_{-10.2}$  pc, indicating that EPIC 228782059 locates farther away from the *Gaia* distance.

To fully establish the observational instability strip of DBV stars, a homogeneous work should be extensively performed to analyze high-quality spectra with serious caution on the hydrogen abundance for known DBVs, including EPIC 228782059, as suggested by Bergeron et al. (2011).

<sup>2</sup> The full time-dependant convection (TDC) and the energy leakage treatment.

The determination of stellar parameters ( $T_{\text{eff}}$  and  $\log g$ ) can be used to map the instability strip of DBV stars, which provides constraints on theoretical expectations.

#### 4. CONCLUSIONS

We report the discovery of 11 independent pulsation modes in the helium-atmosphere pulsating white dwarf (DBV) EPIC 228782059 using more than two months of *K2* photometry. The light curves, spanning nearly 70 d, have been extracted with an optimal 6-pixel aperture and corrected to minimize systematic effects from the spacecraft. We detect 11 frequencies and 2 linear combinations above the  $4.8\sigma$  confidential level. From the average frequency spacing of  $\Delta f \approx 4.0$  and  $6.8 \mu\text{Hz}$  for  $\ell = 1$  and 2 modes, respectively, we measure a rotation period of  $34.1 \pm 0.4$  hr for EPIC 228782059.

With mode identifications from the rotational splittings, a series of grids were constructed using the WDEC evolutionary code based on the atmospheric parameters from spectrum:  $T_{\text{eff}} = 20,868 \pm 160$  K,  $\log g = 7.914 \pm 0.027$  dex (Koester & Kepler 2015). The optimal model of EPIC 228782059 is obtained with a period difference between the theoretical and observed  $m = 0$  modes of 0.131 s. Our asteroseismic solution is similar to the values derived from the SDSS spectrum: we find  $T_{\text{eff}} = 21,910 \pm 23$  K and  $M = 0.685 \pm 0.003 M_{\odot}$  from the *K2* pulsation modes. If this white dwarf truly has  $T_{\text{eff}} < 22,000$  K it would be one of the coolest DBVs known.

The location of EPIC 228782059 on the Kiel diagram can be helpful to test the purity and extent of the DBV instability strip. Our results suggest that EPIC 228782059 is slightly

cooler than the red edge predicted by theoretical calculations (Van Grootel et al. 2017). However, our determinations assume a completely pure helium atmosphere; the presence of even trace amounts of hydrogen could lead to a different  $T_{\text{eff}}$ . We foresee future analysis of this star using higher-resolution spectroscopy, comparison with other seismic models, consideration of various elements in the core as well.

#### ACKNOWLEDGEMENTS

We acknowledge the discussions with Valerie Van Grootel and Bell Keaton which are helpful to improve the manuscript. We acknowledge the support from the National Natural Science Foundation of China (NSFC) through grants 11833002, 11903005, 12090040, 12090042 and 11803004. W.Z. is supported by the Fundamental Research Funds for the Central Universities. J.J.H. acknowledges support provided by NASA *K2* Cycle 6 Grant 80NSSC19K0162. S.C. is supported by the Agence Nationale de la Recherche (ANR, France) under grant ANR-17-CE31-0018, funding the INSIDE project, and financial support from the Centre National d'Études Spatiales (CNES, France). The authors gratefully acknowledge the *Kepler* team and all who have contributed to making this mission possible. Funding for the *Kepler* mission is provided by NASA's Science Mission Directorate.

*Software:* W DEC (Bischoff-Kim & Montgomery 2018), LPCODE (Corsico et al. 2013), Lightkurve (Lightkurve Collaboration et al. 2018), FELIX (Charpinet et al. 2010), MESA (v8118; Paxton et al. 2011; Paxton 2019).

#### REFERENCES

- Althaus, L. G., Córscico, A. H., Isern, J., & García-Berro, E. 2010, *A&A Rv*, 18, 471
- Bailer-Jones, C. A. L., Rybizki, J., Fouesneau, M., Demleitner, M., & Andrae, R. 2021, *AJ*, 161, 147
- Bergeron, P., Wesemael, F., Dufour, P., et al. 2011, *ApJ*, 737, 28,
- Bischoff-Kim, A., & Montgomery, M. H. 2018, *AJ*, 155, 187,
- Bischoff-Kim, A., Østensen, R. H., Hermes, J. J., & Provencal, J. L. 2014, *ApJ*, 794, 39
- Brassard, P., Fontaine, G., & Wesemael, F. 1995, *ApJS*, 96, 545
- Brassard, P., Fontaine, G., Wesemael, F., & Tassoul, M. 1992, *ApJS*, 81, 747
- Charpinet, S., Brassard, P., Giammichele, N., & Fontaine, G. 2019a, *A&A*, 628, L2
- Charpinet, S., Green, E. M., Baglin, A., et al. 2010, *A&A*, 516, L6,
- Charpinet, S., Brassard, P., Fontaine, G., et al. 2019b, *A&A*, 632, A90
- Chidester, M. T., Timmes, F. X., Schwab, J., et al. 2021, *ApJ*, 910, 24
- Córscico, A. H. 2020, *Frontiers in Astronomy and Space Sciences*, 7, 47,
- Córscico, A. H., Althaus, L. G., Miller Bertolami, M. M., & García-Berro, E. 2009, in *Journal of Physics Conference Series*, Vol. 172, *Journal of Physics Conference Series*, 012075
- Córscico, A. H., Althaus, L. G., Miller Bertolami, M. M., & Kepler, S. O. 2019, *A&A Rv*, 27, 7
- Córscico, A. H., Romero, A. D., Althaus, L. G., & Miller Bertolami, M. M. 2013, in *Astronomical Society of the Pacific Conference Series*, Vol. 469, 18th European White Dwarf Workshop., ed. J. Krzesiński, G. Stachowski, P. Moskalik, & K. Bajan, 41
- De Gerónimo, F. C., Battich, T., Miller Bertolami, M. M., Althaus, L. G., & Córscico, A. H. 2019, *A&A*, 630, A100
- Deeming, T. J. 1975, *Ap&SS*, 36, 137
- Dziembowski, W. A., & Goode, P. R. 1992, *ApJ*, 394, 670
- Fontaine, G., & Brassard, P. 2008, *PASP*, 120, 1043
- Fontaine, G., Brassard, P., & Bergeron, P. 2001, *PASP*, 113, 409



- Giammichele, N., Charpinet, S., Fontaine, G., et al. 2018, *Nature*, 554, 73
- Hermes, J. J., Kawaler, S. D., Bischoff-Kim, A., et al. 2017a, *ApJ*, 835, 277
- Hermes, J. J., Gänsicke, B. T., Kawaler, S. D., et al. 2017b, *ApJS*, 232, 23
- Howell, S. B., Sobek, C., Haas, M., et al. 2014, *PASP*, 126, 398
- Kepler, S. O., Nather, E. R., Winget, D. E., et al. 2003, *Baltic Astronomy*, 12, 45
- Kleinman, S. J., Kepler, S. O., Koester, D., et al. 2013, *ApJS*, 204, 5
- Koester, D., & Kepler, S. O. 2015, *A&A*, 583, A86
- Kong, X., Luo, A. L., Li, X.-R., et al. 2018, *PASP*, 130, 084203
- Kritcher, A. L., Swift, D. C., Döppner, T., et al. 2020, *Nature*, 584, 51
- Lamb, D. Q., & van Horn, H. M. 1975, *ApJ*, 200, 306
- Lightkurve Collaboration, Cardoso, J. V. d. M., Hedges, C., et al. 2018, *Lightkurve: Kepler and TESS time series analysis in Python*
- Montgomery, M. H., Provencal, J. L., Kanaan, A., et al. 2010, *ApJ*, 716, 84
- Nather, R. E., Winget, D. E., Clemens, J. C., Hansen, C. J., & Hine, B. P. 1990, *ApJ*, 361, 309
- Niu, J.-S., Li, T., Zong, W., Xue, H.-F., & Wang, Y. 2018, *PhRvD*, 98, 103023
- Østensen, R. H., Bloemen, S., Vučković, M., et al. 2011, *ApJL*, 736, L39
- Paxton, B. 2019, *Modules for Experiments in Stellar Astrophysics (MESA)*, r11701, Zenodo
- Paxton, B., Bildsten, L., Dotter, A., et al. 2011, *ApJS*, 192, 3
- Provencal, J. L., Montgomery, M. H., Kanaan, A., et al. 2009, *ApJ*, 693, 564
- Robinson, E. L., Kepler, S. O., & Nather, R. E. 1982, *ApJ*, 259, 219
- Scargle, J. D. 1982, *ApJ*, 263, 835
- Tassoul, M., Fontaine, G., & Winget, D. E. 1990, *ApJS*, 72, 335
- Timmes, F. X., Townsend, R. H. D., Bauer, E. B., et al. 2018, *ApJL*, 867, L30
- Van Grootel, V., Fontaine, G., Brassard, P., & Dupret, M. A. 2017, in *Astronomical Society of the Pacific Conference Series*, Vol. 509, 20th European White Dwarf Workshop, ed. P. E. Tremblay, B. Gänsicke, & T. Marsh, 321
- Vanderbosch, Z. P., Winget, K. I., & Winget, D. E. 2018, in 21th European White Dwarf Workshop
- Vanderbosch, Z. P., Hermes, J., Agnès Bischoff-Kim, Michael, H. M., & Don, E. 2018, in *Astronomical Society of the Pacific Conference Series*
- Vanderburg, A., & Johnson, J. A. 2014, *PASP*, 126, 948
- Winget, D. E., & Kepler, S. O. 2008, *ARA&A*, 46, 157
- Winget, D. E., Sullivan, D. J., Metcalfe, T. S., Kawaler, S. D., & Montgomery, M. H. 2004, *ApJL*, 602, L109,
- Winget, D. E., van Horn, H. M., Tassoul, M., et al. 1982, *ApJL*, 252, L65
- Zong, W., Charpinet, S., Vauclair, G., Giammichele, N., & Van Grootel, V. 2016, *A&A*, 585, A22